Specificity of the photoreaction of 4'-(hydroxymethyl)-4,5',8-trimethylpsoralen with RNA. Identification of reactive sites in E. coli tRNAPhe

ARTICLE *in* BIOCHEMISTRY · MAY 2002

Impact Factor: 3.02 · DOI: 10.1021/bi00535a039

2 AUTHORS, INCLUDING:

John Hearst
University of California, Berkeley
52 PUBLICATIONS **1,360** CITATIONS

Specificity of the Photoreaction of 4′-(Hydroxymethyl)-4,5′,8-trimethylpsoralen with Ribonucleic Acid. Identification of Reactive Sites in *Escherichia coli* Phenylalanine-Accepting Transfer Ribonucleic Acid†

Jean-Pierre Bachellerie‡ and John E. Hearst*

ABSTRACT: In order to test the potential of psoralen photoaddition for the probing of RNA conformation at sequence resolution, we have analyzed the specificity of the reaction of 4′-(hydroxymethyl)-4,5′,8-trimethylpsoralen (HMT) with *Escherichia coli* $tRNA^{Phe}$. The sites of HMT covalent addition have been identified by a combination of analytical techniques involving chemical cleavage of the $tRNA^{Phe}$ molecule at the m^7G site and gel electrophoresis of RNase T_1 digests together with paper electrophoretic characterization of HMT-modified nucleotides and oligonucleotides. In addition, we have taken advantage of the alteration of the cleavage rate of pancreatic RNase adjacent to a photoadduct. HMT photoaddition shows a very high preference for uracil residues. However, important differences in HMT photoreactivity are observed for various U sites of the $tRNA^{Phe}$ molecule. Reactivity of specific bases has been correlated with partial melting of the molecule. Data available so far indicate a strong preference of the photoreactive probe for a "loose" helical conformation as compared with a tight helix, whereas a random coil appears poorly reactive.

Elucidation of the three-dimensional organization of RNA molecules in solution represents a goal essential for a better understanding of their biological functions. The detailed X-ray crystallographic study of yeast $tRNA^{Phe}$ (Kim et al., 1973; Jack et al., 1976) and the availability of primary sequence data (Sprinzl et al., 1980) have considerably increased our knowledge of the static structure of tRNAs (Rich & RajBhandary, 1976). However, identification of conformational changes, which RNAs could undergo during biological processes, requires more indirect approaches. Thermal unfolding of tRNAs has been studied by a variety of physical approaches involving a combination of melting techniques, nuclear magnetic resonance (NMR) spectroscopy, and relaxation kinetics (Cole et al., 1972; Crothers et al., 1974). The melting process has been shown to result from a number of sequential elementary reorganizations of discrete areas of the molecule. However, detailed information regarding single base residues has been difficult to obtain, even by NMR spectroscopy (Kearns & Schulman, 1974), due to limitations of assigning resonances to individual base pairs. Valuable new information about local conformations can be generated by using a number of different probes, like structure-specific nucleases (Wurst et al., 1978; Ross & Brimacombe, 1979), oligonucleotide binding (Uhlenbeck et al., 1974), and chemical modifications of RNA (Litt, 1969; Goddard & Lowdon, 1978; Rhodes, 1977; Wagner & Garrett, 1978). We have undertaken a study to test the potential usefulness of the psoralen photoreaction to probe RNA structure in solution [see Thompson et al. (1982)]. In this study, we have chosen *Escherichia coli* $tRNA^{Phe}$ (Figure 1) as a model system for analyzing the specificity of the photoaddition of (hydroxymethyl)trimethylpsoralen (Isaacs et al., 1977).

Experimental Procedures

Materials. E. coli $tRNA^{Phe}$ was obtained from Boehringer-Mannheim. RNase T_2 (EC 3.1.23) was purchased from Sigma. Pancreatic RNase A (EC 2.7.7.16) and calf intestine alkaline phosphatase (EC 3.1.3.1) were Boehringer-Mannheim products. RNase T_1 (EC 2.1.48) was obtained from Sankyo. [^{3}H]HMT[1] (3.7×10^7 cpm/μg) was synthesized by S. Isaacs of this lab according to Isaacs et al. (1982). Aniline was distilled in the presence of zinc powder under reduced nitrogen pressure and stored at −20 °C in the dark.

Photoreaction. Samples to be irradiated were put in glass tubes and irradiated in an apparatus described previously (Bachellerie et al., 1981). Samples contained 200 μg/mL tRNA and 20 μg/mL HMT. Unless otherwise noted, samples contained 1 mM Tris-HCl, pH 7.4, and 0.1 mM EDTA and were irradiated for 15 s at 5 °C. The light intensity at the surface of the sample was approximately 100 mW/cm^2. After irradiation, RNA samples were extracted twice with phenol and then ethanol precipitated 3 times to remove unbound HMT. Full-size irradiated $tRNA^{Phe}$ was further purified by electrophoresis on a 10-cm 20% polyacrylamide–7 M urea slab gel run in 50 mM Tris–borate, pH 8.3, and 1 mM EDTA for 12 h at 250 V. It was visualized by placing the preparative gel on a cellulose sheet containing fluorescent indicator and briefly illuminating the gel with short-wavelength UV light. (This causes less than 2% reversal of the HMT adducts.) The band was excised from the gel and RNA eluted from the crushed polyacrylamide by 0.3 M NaCl (6 h at 0 °C). Eluted RNA was then phenol extracted and ethanol precipitated. It could be stored for months in a stable form at −20 °C in the dark. During subsequent analysis, special care was taken to minimize UV light exposure of the sample, which could result

† From the Department of Chemistry, University of California, Berkeley, Berkeley, California 94720. *Received May 18, 1981.* This work was supported in part by National Institutes of Health Grant GM 11180, by an NIH Fogarty Fellowship to J.-P.B., and by the Assistant Secretary for Environment, Office of Environmental Research and Development, Biomedical and Environmental Research Division of the U.S. Department of Energy under Contract No. W-7405-ENG-48.

‡ Present address: Centre de Recherche de Biochimie et Génétique Cellulaires du CNRS, 31062 Toulouse Cedex, France.

[1] Abbreviations: HMT, 4′-(hydroxymethyl)-4,5′,8-trimethylpsoralen; Tris, tris(hydroxymethyl)aminomethane; EDTA, ethylenediaminetetraacetic acid; PEI, poly(ethylenimine); CD, circular dichroism; RNase, ribonuclease.

0006-2960/82/0421-1357$01.25/0

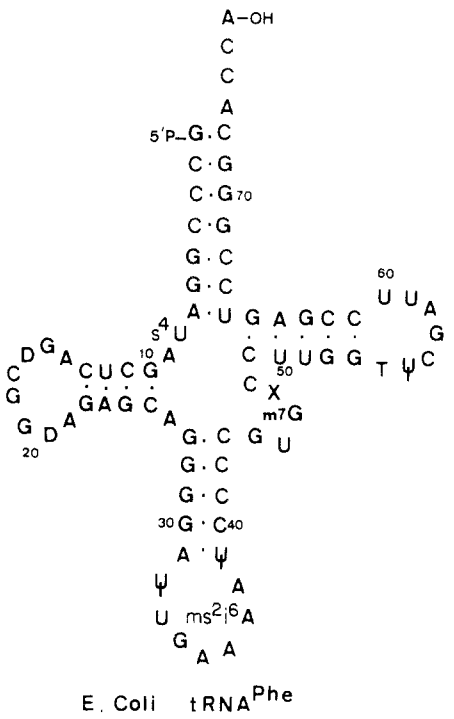

FIGURE 1: Nucleotide sequence and cloverleaf structure of *E. coli* phenylalanine-accepting tRNA.

in the reversal of HMT photoaddition (Bachellerie et al., 1981).

Chemical Cleavage of tRNA^{Phe} at m^{7}G. This was performed according to Wintermeyer & Zachau (1975). Aniline cleavage products (tRNA^{Phe} fragments "1–45" and "47–76") were separated by electrophoreses in 20% polyacrylamide–7 M urea slab gels and were detected both by ethidium bromide fluorescence and by ^{3}H radioactivity profiles. For subsequent analysis, tRNA^{Phe} fragments were recovered from the gel as described above for intact tRNA^{Phe}.

5′-End Labeling of the 47–76 Fragment. The purified 47–76 fragment (1–2 μg) was dephosphorylated by 2.5 milliunits of calf alkaline phosphatase in 50 mM Tris-HCl, pH 8.3 (1 h, 37 °C). After several phenol extractions followed by ether extraction, phosphorylation was achieved according to Donis-Keller et al. (1977) in 50 mM Tris-HCl, pH 9.0, 10 mM $MgCl_2$, 5 mM dithiothreitol, 75 μM ATP (containing 75 μCi of [γ-^{32}P]ATP), and 6 units of T_4 polynucleotide kinase (reaction volume 20 μL, 45-min incubation at 37 °C). The reaction was stopped by adding 5 μL of 50 mM EDTA, pH 8.0, and the incubation mixture was loaded onto a 20% polyacrylamide–7 M urea slab gel in 50 mM Tris–borate, pH 8.3, and 1 mM EDTA after addition of an equal volume of 10 M urea, 0.05% xylene cyanol, and 0.05% bromophenol blue. After a 6-h migration at 1100 V, the gel was autoradiographed. The expected band for the 30 nucleotide long fragment was the only detectable ^{32}P-labeled material on the gel (except ATP and ATP degradation products, which migrated faster than bromophenol blue dye). The gel around the ^{32}P-labeled peak was cut into 1-mm slices and the RNA eluted with 0.3 M NaCl (6 h, 0 °C). The ^{3}H radioactivity profile, obtained from aliquots of the eluted fractions, showed a unique peak almost exactly coincident with the ^{32}P radioactivity peak (a 1-mm shift was actually observed, due to the retardation effect of HMT adduct). Eluted peak fractions were phenol extracted and ethanol precipitated before subsequent analysis.

The identification of the faster moving m^{7}G cleavage RNA fragment as the 47–76 segment was confirmed by sequencing-gel analysis of the partial RNase T_1 digest of the 5′ (^{32}P) fragment performed according to Donis-Keller et al. (1977). The observed sequence was 5′P-N_5GGN_3GN_5GNGN_3G-GGN_5-3′OH (with N being A, C, or U) as expected for the 47–76 fragment.

Enzyme Digestions. Complete RNase T_1 digests were obtained from full-size tRNA^{Phe} or from fragments 1–45 and 47–76 by a 3-h incubation at 37 °C in 25 mM Tris-HCl, pH 7.4, and 10 mM EDTA with an enzyme/substrate ratio of 1:20 (w/w).

Pancreatic RNase digestions of T_1 oligonucleotides were performed (2 h at 37 °C) at variable enzyme/substrate ratios as described in Figure 5. RNase T_2 digestions were carried out by overnight incubation at 37 °C in 50 mM $NaC_2H_3O_2$, pH 5 (1 unit/5 μg of RNA).

Analysis of Oligonucleotides. RNase T_1 digests were run on 20% polyacrylamide–7 M urea slab gels (40 cm high, 0.6 mm thick) in 50 mM Tris–borate, pH 8.3, and 1 mM EDTA for 12 h at 1000 V. ^{3}H radioactivity profiles were determined by liquid scintillation counting on aliquots of 2-mm gel slices after oligonucleotide elution from each crushed slice with 0.3 M NaCl. Eluted fractions were dialyzed against H_2O and freeze-dried before subsequent analysis, either directly by gel electrophoresis at pH 3.5 or by paper electrophoresis after pancreatic RNase digestion.

The 10% polyacrylamide–6 M urea slab gels were run at pH 3.5 according to De Wachter & Fiers (1972).

5′-End Group Analysis. 5′-^{32}P-Labeled oligonucleotides were digested with RNase T_2. 5′-^{32}P-Labeled nucleoside 3′,5′-diphosphates were analyzed by chromatography on PEI–cellulose sheets in 1.75 M ammonium formate and in 0.55 M ammonium sulfate (Gupta & Randerath, 1979).

Paper Electrophoresis. Paper electrophoresis was performed at pH 3.5 (in 5% acetic acid and 0.5% pyridine) on Whatman No. 1 paper as described elsewhere (Bachellerie et al., 1981), in the presence of ^{32}P-labeled mononucleotide markers.

Results

Overall Reactivity of E. coli tRNA^{Phe}. The analysis of HMT-reacted tRNA^{Phe} on 20% polyacrylamide–7 M urea gels showed that no detectable breakdown of tRNA^{Phe} occurred during photoreaction. In these conditions, [^{3}H]HMT-labeled tRNA^{Phe} migrated as a homogeneous band, coincident with unreacted [5′-^{32}P]tRNA^{Phe}, even for very long runs. Transfer RNA material migrating in this band appeared more than 95% pure. Sequencing-gel analysis of RNase T_1 partial digests of [5′-^{32}P]tRNA^{Phe} performed according to Donis-Keller et al. (1977) showed a pattern of G sites in line with the complete sequence determined by Barrell & Sanger (1969). However, some sequence heterogeneity at the X nucleoside position was revealed by the gel band pattern as will be discussed below.

Uracil Is the Major Photoreactive Base. HMT-modified nucleotides, which are formed upon irradiation, can be umambiguously identified by electrophoresis on Whatman No. 1 paper at pH 3.5 after complete hydrolysis of the RNA phosphodiester chain. Mobilities of all possible products of HMT monoaddition or cross-linkage on model compounds (mono- and dinucleotides, homo- and copolynucleotides) have been experimentally determined in studies published elsewhere (Bachellerie et al., 1981; Thompson et al., 1982; J.-P. Bachellerie and J. E. Hearst, unpublished results).

For all conditions of photoreaction of tRNA^{Phe} tested so far, more than 95% of [^{3}H]HMT adduct migrated as a major peak (R_f = 0.62) with a minor shoulder (R_f = 0.58) after RNase T_2 hydrolysis (results not shown). These species have been shown (Bachellerie et al., 1981) to correspond to different isomers of uridine monophosphate monoadduct. A very minor

Table I: List of U or U Analogue Containing Oligonucleotides Produced by T_1 RNase from *E. coli* $tRNA^{Phe}$ according to Barrell & Sanger (1969)

oligonucleotides produced by T_1 RNase	location after m^7G chemical cleavage: fragment 1–45	fragment 47–76
$^{35}AAms^2i^6AA\Psi CCCC^{44}Gp$ (a)	+	
$^{45}Um^7GXCCUU^{52}Gp$ (b)	^{45}UpK [a]	$^{47}5'pXCCUU^{52}Gp$ [b]
$^{58}AUUCC^{63}Gp$ (c)		+
$^{11}CUCA^{15}Gp$ (d)	+	
$^{7}As^4UA^{10}Gp$ (e)	+	
$^{31}A\Psi U^{34}Gp$ (f)	+	
$^{54}T\Psi C^{57}Gp$ (g)		+
$^{66}UCC^{69}Gp$ (h)		+

[a] K denotes the elimination product of the ribose moiety of m^7G. [b] X is 3-(3-amino-3-carboxypropyl)uridine; note that m^7G chemical cleavage produces a 5'-phosphorylated 47–76 fragment.

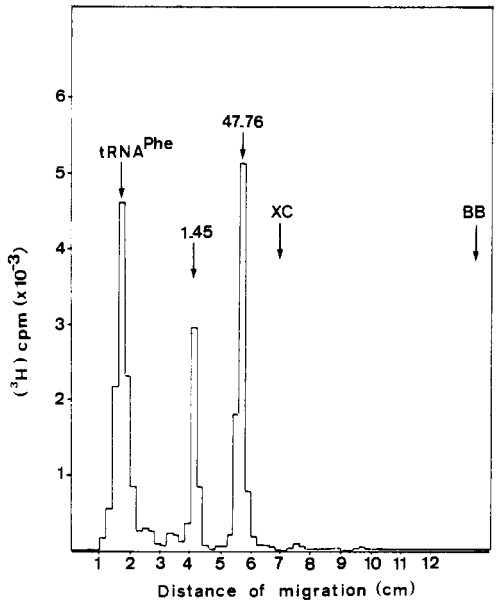

FIGURE 2: Polyacrylamide gel electrophoresis of [^{3}H]HMT-photoreacted $tRNA^{Phe}$ after cleavage at m^7G. [^{3}H]HMT-photoreacted $tRNA^{Phe}$ was purified and cleaved by aniline after $NaBH_4$ reduction. Reaction products were analyzed on a 20% polyacrylamide–7 M urea gel and detected in separate lanes by ethidium bromide fluorescence (not shown) and ^{3}H radioactivity (2-mm gel slices were treated overnight with 1.5 N NH_4OH before liquid scintillation counting). Positions of dye markers [xylene cyanol (XC) running like a 25-mer and bromophenol blue (BB) like an 8-mer] are indicated by arrows.

slow-moving peak (R_f = 0.10) could either correspond to a monoadduct of cytidine (R_f = 0.14) (Bachellerie et al., 1981) or to an HMT breakdown product that is not removed by the purification. It has been observed that the uridine analogues present in $tRNA^{Phe}$ (Ψ, D, s^4U) are much less reactive than uridine (Bachellerie et al., 1981).

Identification of RNase T_1 Resistant Oligonucleotides Containing an HMT Monoadduct. We found that the identification of the HMT-reactive oligonucleotides (listed in Table I) could be greatly facilitated by the specific chemical cleavage reaction (Wintermeyer et al., 1972; Wintermeyer & Zachau, 1975) of the $tRNA^{Phe}$ molecule at the site occupied by m^7G (position 46 from the 5' end).

Fragments 1–45 and 47–76 were prepared from [^{3}H]-HMT-photoreacted $tRNA^{Phe}$ and purified by polyacrylamide gel electrophoresis (Figure 2). The cleavage reaction was about 55% effective on [^{3}H]HMT-photoreacted molecules, a value very similar to that obtained for unmodified 5'-^{32}P-end-labeled $tRNA^{Phe}$ (not shown). No ^{3}H radioactivity could

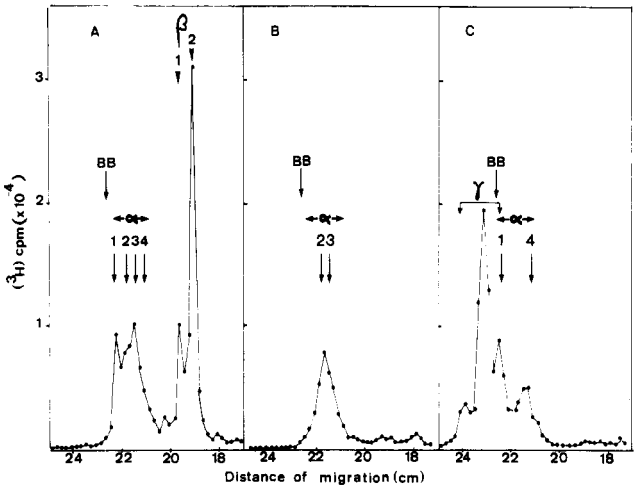

FIGURE 3: Polyacrylamide gel electrophoresis of a complete RNase T_1 digest of material from the three [^{3}H]HMT-labeled peaks of Figure 2. Full-size $tRNA^{Phe}$, the 1–45 fragment, and the 47–76 fragment resulting from m^7G cleavage were extracted from the gel of Figure 2, purified, and extensively digested with RNase T_1 as described under Experimental Procedures. The incubation mixtures were made 7 M with urea and run on a thin 20% polyacrylamide–7 M urea gel (40 cm × 20 cm × 0.6 mm) for 6 h at 1000 V. ^{3}H radioactivity profiles were determined by liquid scintillation on 2-mm gel slices after an overnight treatment with 1.5 N NH_4OH in order to obtain full counting efficiency. Total gel lanes were analyzed but radioactivity was exclusively located in the area shown here. The position of the bromophenol blue (BB) marker is indicated by the arrow. (A) Full-size $tRNA^{Phe}$; (B) 1–45 fragment; (C) 47–76 fragment.

be detected other than at the positions of the 1–45 and 47–76 fragments and of the intact $tRNA^{Phe}$, indicating that [^{3}H]-HMT labeling remained quantitatively bound to RNA throughout the cleavage reaction and that no additional cleavage resulted from the presence of HMT adducts. About 65% of bound [^{3}H]HMT in cleaved $tRNA^{Phe}$ was recovered in the small 47–76 fragment (Figure 2).

Characterization of $Um^7GXCCUUG$ as the Major HMT-Reactive RNase T_1 Resistant Oligonucleotide. Figure 3 shows the ^{3}H radioactivity pattern obtained upon polyacrylamide gel electrophoresis of RNase T_1 digests of the [^{3}H]HMT-photoreacted $tRNA^{Phe}$ and of the 1–45 and 47–76 fragments. Two groups of ^{3}H-labeled oligonucleotides were resolved from $tRNA^{Phe}$ (Figure 3). Identical ^{3}H radioactivity profiles were obtained after T_1 RNase digests of HMT-photoreacted $tRNA^{Phe}$ either untreated or treated and resistant to m^7G chemical cleavage. The slower migrating "β" group contained a major "β_2" and a minor "β_1" component, whereas four subcomponents could be clearly detected in the "α" group (results of longer migrations not shown). The β-group components were not detected in RNase T_1 digests of either 1–45 or 47–76 fragments, suggesting that the m^7G cleavage site was located within the oligonucleotides of the β group. A new group ("γ") of ^{3}H-labeled RNase T_1 resistant oligonucleotides, migrating faster than the β group, was produced in digests of the 47–76 fragment. The amount of ^{3}H counts recovered in γ_1 and γ_2 peaks was very close to what was measured in the β_1 and β_2 peaks, respectively, when RNase T_1 digestion was carried out on corresponding quantities of intact $tRNA^{Phe}$. On this basis, the β group has been assigned to the fragment $Um^7GXCCUUG$. The T_1 RNase digest of the 5'-^{32}P-labeled 47–76 fragment from [^{3}H]HMT-photoreacted $tRNA^{Phe}$ was analyzed on sequencing acrylamide gels at conditions identical with those described for Figure 3. All of the ^{32}P was found either at the position of the unmodified XCCUUG or at the ^{3}H-labeled γ group (results not shown). On this basis, the γ group has been assigned to the fragment XCCUUG. The

Table II: Electrophoretic Mobilities of Dinucleotide HMT Photoproducts at pH 3.5 [a]

HMT monoadduct of dinucleotide mono-P	predicted R_f	obsd R_f	HMT monoadduct of dinucleotide (3′P) di-P	predicted R_f	obsd R_f
UpU	0.52	0.54 [b] 0.50	UpUp	0.96	0.95 [b] 0.90
UpG	0.44	0.45 [b] 0.43	UpGp	0.87	0.84 [b] 0.82
UpA	0.25	0.25 [b] 0.20	UpAp	0.70	nd [c]
UpC	0.13	0.11	UpCp	0.60	0.53
control dinucleotide mono-P	predicted R_f	obsd R_f	control dinucleotide (3′P) di-P	predicted R_f	obsd R_f
UpU	0.67	0.65	UpUp	1.21	nd
UpG	0.56	0.55	UpGp	1.08	nd
UpA	0.32	0.32	UpAp	0.87	nd
UpC	0.17	0.16	UpCp	0.74	nd

[a] The predicted mobilities were calculated from the equation $R_f = -45.4(Q/M_r^{2/3})$, where Q is the net charge and M_r is the molecular weight. m^7G is the reference [$R_f(m^7G) = -1$] according to Sommer (1979). [b] Two different stereochemical products were resolved. [c] nd means not determined.

$^{32}P/^{3}H$ count ratio remained roughly constant throughout the γ-group area: its average value of 8.0 corresponded approximately to what would be predicted for oligonucleotides containing HMT and 5′-terminal phosphate in a 1:1 molar ratio (1 pmol of [^{3}H]HMT corresponded to 10^4 cpm, and [^{32}P]ATP was 45 Ci/mmol). On the other hand, no ^{32}P radioactivity was found comigrating with the slower ^{3}H-labeled α_4 peak.

Identification of the HMT-Reactive Sites. An extensive digestion of the β group, $Um^7GXCCUUGp$, by pancreatic RNase should give rise to m^7GXCp, Cp, Gp, and three Up. We observed, however, in studies using [^{3}H]HMT-photoreacted model oligonucleotides (J.-P. Bachellerie and J. E. Hearst, unpublished results) that the presence of an HMT monoadduct dramatically inhibits the cleavage by pancreatic RNase of the phosphodiester bond adjacent (3′ side) to the modified uracil, while a much lower but significant inhibition could be measured for the cleavage of the 5′-pyrimidine–p(U)* bond. This property was particularly helpful for identifying modified U's among several potentially reactive sites as was the case in $Um^7GXCCUUGp$.

The possibility that ^{45}U was the unique photoreactive site in $Um^7GXCCUUGp$ oligonucleotide could be ruled out from results shown in Figure 2 indicating that most, if not all, of the HMT in $Um^7GXCCUUGp$ was located beyond m^7G in the 5′ to 3′ direction.

In order to discriminate between the three remaining pancreatic digestion products, (X)*pCp, ^{50}(U)*pUp, or ^{51}(U)*pGp (where the asterisked parenthesized base denotes the HMT-modified nucleotide), we performed a systematic characterization of all possible U-containing dinucleotides after photoaddition of [^{3}H]HMT by paper electrophoresis at pH 3.5. The mobilities of these products (either as mono- or diphosphates) are listed in Table II. Experimental values were in close agreement with theoretical R_f's calculated from an empirical equation used to predict the electrophoretic mobility of nucleotides on paper (Sommer, 1979). For a given U-containing dinucleotide, more than one HMT photoproduct could generally be separated (Table II). They have been shown to correspond to different HMT stereoisomers of slightly different R_f, but the average R_f value of the set of isomers was very similar to the predicted value. Since a much better resolution could be achieved in the dinucleotide monophosphate form (see Table II), pancreatic RNase digests of the HMT-modified $Um^7GXCCUUGp$ oligonucleotide were also analyzed after dephosphorylation by alkaline phosphatase. When pancreatic RNase digestion was carried out at sufficient concentration (10 times the concentration usually necessary to hydrolyze every phosphodiester bond on the 3′ side of unmodified pyrimidines), only one ^{3}H-labeled species was detected by paper electrophoresis, comigrating exactly with either (U)*pGp (Figure 4) or Up(U)*pG (Figure 4c). Its conversion into (U)*pG at higher enzyme/substrate ratio was also in line with this species being Up(U)*G, the Up(U)* phosphodiester linkage being partially resistant to pancreatic RNase at lower enzyme/substrate ratio (Figure 4a,b) (J.-P. Bachellerie and J. E. Hearst, unpublished results). Only a small proportion (less than 5%) of the ^{3}H counts migrated as (U)*pU (the small peak near 20 cm in Figure 4d), indicating a very low level of HMT photoreactivity for ^{50}U as compared with ^{51}U.

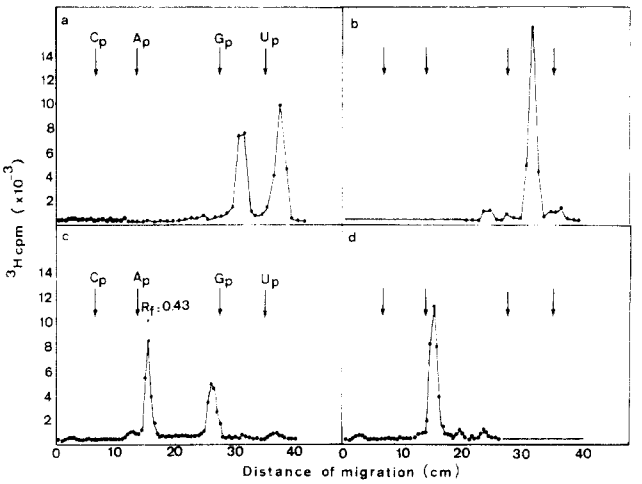

FIGURE 4: Paper electrophoresis of pancreatic RNase digests of the HMT-modified $Um^7GXCCUUGp$ oligonucleotide from photoreacted $tRNA^{Phe}$. [^{3}H]HMT-labeled $Um^7GXCCUUGp$ was prepared by polyacrylamide gel electrophoresis of a complete T_1 RNase digest of photoreacted $tRNA^{Phe}$ as shown in Figure 3. The eluted fragment from the gel was dialyzed and lyophilized. The fragment was digested (2 h, 37 °C, in 10 mM Tris-HCl, pH 7.4, and 0.4 mM EDTA) by increasing amounts of pancreatic RNase in the presence of a constant concentration of unlabeled tRNA carrier (0.4 μg/μL). After the reaction, half of each digest was immediately analyzed by electrophoresis on Whatman No. 1 paper at pH 3.5 while the remaining half was added to an equal volume of 50 mM Tris, pH 8.3, and 1.25 mM $ZnSO_4$ and digested for an additional 1 h at 37 °C with 0.2 unit of calf intestine alkaline phosphatase. (a and b) Direct analysis of pancreatic RNase digests obtained with RNA/enzyme (w/w) ratios of 20:1 (a) or 20:10 (b); (c and d) ^{3}H profiles after dephosphorylation by alkaline phosphatase of pancreatic RNase digests obtained with RNA/enzyme (w/w) ratios of 20:1 (c) or 20:10 (d).

Identification of the "Minor" HMT-Photoreactive Sites. [^{3}H]HMT-labeled oligonucleotides migrating in the α area of 20% acrylamide, pH 8.3, gels (Figure 3) were clearly resolved by longer migrations (on the average, 35 cm) into four subcomponents termed α_1, α_2, α_3, and α_4, which were extracted from the gel and analyzed further. Each of these subcomponents appeared homogeneous when electrophoresed on 10% acrylamide–6 M urea gels at pH 3.5 at conditions (De Wachter & Fiers, 1972) allowing for the separation of short oligonucleotides of the same size but different (U + G)/(C + A) ratios (not shown). Pancreatic RNase digestions were carried out on each purified subcomponent, and resistant [^{3}H]HMT-labeled products were identified by paper electrophoresis at pH 3.5, as described above (Figure 4, Table II). Results are listed in Table III. A 5′ end group analysis was

Table III: Identification of HMT-Photoreactive Sites in Oligonucleotides Produced by T_1 RNase

T_1 RNase oligonucleotide	T_1 + pancreatic RNase HMT-modified products [a]	location after m^{7}G cleavage [b]	proposed identification of HMT-modified oligonucleotide	relative amount of HMT addition (with $^{51}U = 1.0$)
1	(U)*C	47–76	(U)*CCG [c] [or T(Ψ)*CG]	$^{66}U = 0.2$ (or Ψ)
2	(U)*G	1–45	A(U)*G	$^{33}U = 0.2$
3	(U)*C	1–45	C(U)*CAG	$^{12}U = 0.3$
4	(U)*C + (U)*U	47–76	AU(U)*CCG, A(U)*UCCG	$^{60}U = 0.05$, $^{59}U = 0.05$

[a] Identification of [^{3}H]HMT-labeled pancreatic RNase products from oligonucleotides was carried out as described in the legend to Figure 4. [b] Results of an experiment similar to that described by Figure 2. [c] Since (Ψ)*C should not be separated from (U)*C by paper electrophoresis at pH 3.5, α_1 could also correspond to T(Ψ)*CG. However, this appears unlikely, considering the mobility of α_1 on acidic pH gel (not shown) and also the very low HMT photoreactivity of Ψ measured with model systems (Bachellerie et al., 1981).

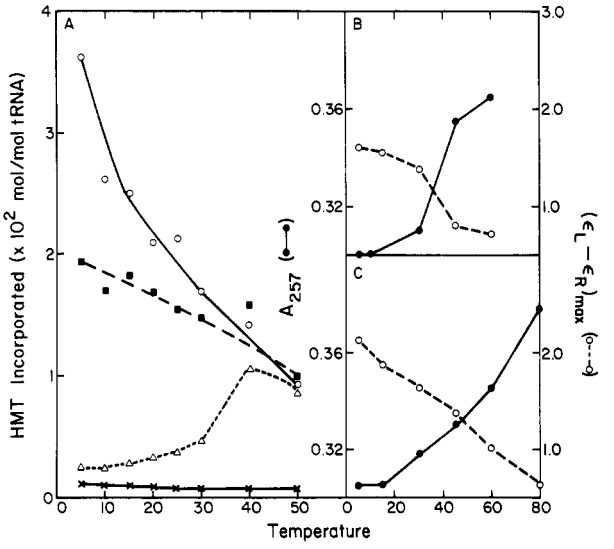

FIGURE 5: (A) Temperature dependence of HMT addition to *E. coli* $tRNA^{Phe}$ at 1 mM Tris-HCl, pH 7.4, and 0.1 mM EDTA and no salt (○), 5 mM NaCl (■), 100 mM NaCl (△), and 5 mM NaCl and 5 mM $MgCl_2$ (×). (B) $(\epsilon_L - \epsilon_R)_{max}$ for *E. coli* $tRNA^{Phe}$ with no added salt (○) and absorbance at 257 nm (●). (C) $(\epsilon_L - \epsilon_R)_{262}$ for *E. coli* $tRNA^{Phe}$ at 100 mM NaCl (○) and absorbance at 257 nm (●).

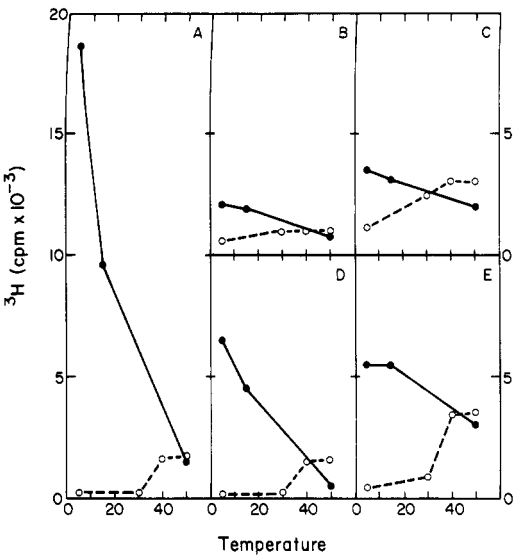

FIGURE 6: Temperature dependence of HMT addition to (A) ^{51}U, (B) $^{59,60}U$, (C) ^{33}U, (D) ^{66}U, (E) ^{12}U with 1 mM Tris, pH 7.4, and 0.1 mM EDTA and no added salt (●) or 100 mM NaCl (○).

also performed on the α_4 oligonucleotide, which could be obtained from the 47–76 fragment of [^{3}H]HMT-photoreacted $tRNA^{Phe}$. After 5′-^{32}P-end labeling, the α_4 oligonucleotide was repurified by 25% acrylamide–7 M urea gel electrophoresis, extracted from the gel, and hydrolyzed by RNase T_2. Upon chromatography on a PEI–cellulose sheet according to Gupta & Randerath (1979), this digest revealed only one labeled spot comigrating with 5′pA3′p in both solvent systems. This identifies α_4 as AUUCCG, which is the only RNase T_1 resistant oligonucleotide possessing a 5′-terminal A in the 47–76 fragment of $tRNA^{Phe}$.

Conformation Dependence of HMT Addition. The rate of HMT incorporation into *E. coli* $tRNA^{Phe}$ is shown as a function of salt and temperature in Figure 5. The temperature dependence of addition at 100 mM NaCl is noteworthy in that addition is actually substantially increased as the temperature is raised from 20 to 40 °C. Large changes in the UV and CD spectra were also observed [Figure 5B,C; see Thompson et al. (1982) (accompanying paper) for experimental details]. The salt and temperature dependence of addition to specific bases was also studied (Figure 6). The most reactive base, ^{51}U, was also the most sensitive to temperature at low salt.

Discussion

Conditions of Photoreaction. In this work we have studied the specificity of HMT photo*mono*addition on $tRNA^{Phe}$. Since cross-link formation is a two-photon event (Johnston et al., 1977; Johnston & Hearst, 1981), low light dose irradiations favoring monoaddition were performed in the presence of maximum HMT concentrations. In our pulse irradiation conditions, the amount of covalently bound HMT corresponded to about 10% of the plateau value obtained with long irradiation. The rate of photoaddition remained linear throughout the pulse period. Paper electrophoresis of T_2 RNase digests of photoreacted $tRNA^{Phe}$ confirmed the absence of the most frequently occurring cross-linked nucleotide in RNA (U–U cross-link, $R_f = 0.99$), which we characterized in a previous study (Bachellerie et al., 1981).

Another reason for the choice of low doses of light for photoreaction results from the observation (Yaniv et al., 1969; Favre et al., 1977) that 335-nm light can induce the formation of a covalent linkage in tRNAs between 4-thiouridine and cytidine (in positions 8 and 13 from the 5′ end, respectively). We observed the production of significant amounts of s^4U–C cross-linked $tRNA^{Phe}$ for longer irradiation periods. This cross-linked species was produced in negligible amounts during a 15 s pulse irradiation. The cross-linked product was also clearly separated from main-band $tRNA^{Phe}$ by the preparative acrylamide gel electrophoresis. Consequently, this cross-linking process did not interfere with identification of HMT-photoreactive sites.

It is interesting to note here that we observed an overall HMT photoreactivity about 50% higher for s^4U–C cross-linked $tRNA^{Phe}$ than for $tRNA^{Phe}$ at identical irradiation conditions (low temperature, no or low salt). This seems to indicate a better accessibility for the drug to some uracil residue(s) subsequent to s^4U–C cross-linking.

Identification of HMT Reactive Sites in tRNA^{Phe}. We took advantage of a rather simple spectrum of RNase T_1 resistant U-containing (or U analogue containing) oligonucleotides in tRNA^{Phe} (Table I) and of an even simpler spectrum of [^{3}H]HMT-modified T_1 oligonucleotides (Figure 2). However, their analysis was hindered by two major difficulties. We chose to produce only a low degree of HMT photoaddition, which means that HMT-modified RNase T_1 oligonucleotides represented a small fraction (0.5–5%) of their unmodified counterparts. On the other hand, the HMT photoaddition results in modified electrophoretic behavior of the oligonucleotides (the shorter the fragment, the more marked the effect) with the possible overlap of modified and unmodified oligonucleotides of different sizes and compositions. For example, β-group components migrated like a 10–11 nucleotide long unmodified fragment. Using the same psoralen derivative, Thompson et al. (1981) made similar observations. The identification of the β oligonucleotide as Um^{7}GXCCUUGp was also complicated by the significant sequence heterogeneity we observed in tRNA^{Phe} at the X nucleoside position. Ohashi et al. (1974) characterized the X nucleoside as 3-(3-amino-3-carboxypropyl)uridine while detecting the presence of significant amounts (about 20%) of a closely related nucleoside. In our study, PEI–cellulose chromatography resolved pXp into one major (about 70%) and two minor bands (each about 15% and one behaving like uridine in two solvent systems) moving slightly ahead of the major band. As a consequence HMT-modified Um^{7}GXCCUUGp was resolved into subcomponents of slightly different mobilities on acrylamide gels. No ^{3}H-labeled species migrating slower than Um^{7}GXCCUUGp on a 20% acrylamide–7 M urea gel after RNase T_1 digestion of tRNA^{Phe} could be detected, indicating no significant HMT photoreactivity of nucleotides located from position 35 to 44.

The identification of (U)*pG as the almost exclusive pancreatic RNase resistant HMT-modified product from Um^{7}GXCCUUGp (Figure 6) demonstrated that ^{51}U was the major HMT-photoreactive site in tRNA^{Phe}, binding approximately 50% of HMT covalently bound to this molecule at 5 °C in the absence of salt. Outside the Um^{7}GXCCUUG region, a significant HMT photoaddition was observed for every U in the tRNA^{Phe} molecule even though all these sites were clearly less reactive than ^{51}U (Table III). These sites are located either in helical stems (^{12}U and ^{66}U) or at a UU or a ΨU site at the end of a stem.

Conformation Dependence. The transitions observed with both the HMT incorporation and the optical properties are, in general, not as sharp with tRNA as they are with synthetic polymers. This is caused by the greater variety of interactions in tRNA. A "phase diagram" for the structure of a number of *E. coli* tRNAs (including Phe) has been developed on the basis of temperature-jump experiments (Cole et al., 1972). In these experiments, Mg^{2+} was carefully removed and the optical transitions observed are virtually identical with ours. In these magnesium-deficient conditions, the tertiary structure melts first.

The smooth decreases observed in HMT incorporation with 5 mM NaCl and 5 mM Tris–EDTA are paralleled by changes in the optical properties; however, they cannot be assigned to specific conformational changes. With 100 mM NaCl, it is clear from the optical properties that changes in structure are occurring around 30 °C.

The phase diagram developed by Cole et al. (1972) for *E. coli* tRNA^{Phe} predicts melting of the native tertiary structure at about 35 °C. This melting makes the molecule considerably more flexible and makes intercalation easier. This is clear from the sharp increase (275%) in HMT incorporation. The greatest increase is observed with ^{12}U. When the tertiary structure is present, ^{12}U is located in a rigid region with several tertiary interactions nearby. Once these interactions have melted, ^{12}U is in a short helix, which allows easy intercalation. ^{51}U and ^{66}U also increase in reactivity, but not as sharply. Both of these bases are also in helices that allow better intercalation once the tertiary constraints have been removed. ^{51}U and ^{66}U are each different from ^{12}U in very important respects. ^{66}U is at the end of a helix. ^{51}U is part of a G–U pair. Since this pair is relatively unstable, it seems reasonable to predict that it would allow intercalation to occur more readily. It will be necessary to examine more systems in order to separate these different structural effects.

^{33}U increases in reactivity much more gradually. Since the anticodon loop is not directly affected by the tertiary structure, it is not suprising that there is no sharp transition. The stacking in the anticodon loop must be disrupted sufficiently at higher temperatures to allow better intercalation. There is virtually no change in the reactivity of ^{59,60}U with temperature. These bases interact only minimally with the rest of the molecule.

Analysis of the temperature depenence in Tris–EDTA is a more complex problem. In these conditions there is evidence that neither the native structure nor the cloverleaf form exists at any temperature. The lack of cations increases the repulsion between the phosphates so much that an open or extended structure is the most stable. A model based on temperature-jump studies has been proposed (Cole et al., 1972), but no other methods have been used to test the validity of this model. This makes it difficult to relate the reactivity of the different bases to their conformation. In this "extended" form model, ^{33}U and ^{59,60}U are both in unpaired regions. They show little change in reactivity with temperature. The higher reactivity of ^{33}U is probably caused by the greater degree of base stacking in the anticodon loop. ^{66}U, in the acceptor stem, shows a large drop in reactivity with temperature. Presumably, this occurs as the acceptor stem melts. ^{51}U is postulated to be in a G–U pair at the end of a weak helix. This would melt quickly and yield the sharp temperature dependence observed. Determining the exact structure of this region would certainly be worthwhile since this is by far the most reactive site in the molecule in these conditions. ^{12}U is more difficult to rationalize. It is assigned to an unpaired region, but it is possible to base pair it by extending the acceptor stem with bases 11–13 and 63–65. This would force ^{8}s^{4}U into a bulge. There is absorption evidence that indicates it is paired, however. If ^{12}U is paired as suggested above, a temperature dependence more like ^{66}U would be expected.

Conclusions

From this study and the accompanying one (Thompson et al., 1982), it is obvious that certain types of helical structure accelerate the reaction of HMT with RNA. Changes in the rate of HMT incorporation could not be perfectly predicted by optical properties. The salt and temperature dependence of HMT incorporation was more complex than for synthetic polymers (Thompson et al., 1982), but the differences are readily explainable by known aspects of tRNA structure.

References

Bachellerie, J. P., Thompson, J. F., Wegnez, M., & Hearst, J. E. (1981) *Nucleic Acids Res. 9*, 2207–2222.

Barrell, B. G., & Sanger, F. (1969) *FEBS Lett. 3*, 275–278.

Cole, P. E., Yang, S. K., & Crothers, D. M. (1972) *Biochemistry 11*, 4358–4368.

Crothers, D. M., Cole, P. E., Hilbers, C. W., & Schulman, R. G. (1974) *J. Mol. Biol. 87*, 63–88.
De Wachter, R., & Fiers, W. (1972) *Anal. Biochem. 49*, 187–197.
Donis-Keller, H., Maxam, A. M., & Gilbert, W. (1977) *Nucleic Acids Res. 4*, 2527–2538.
Favre, A., Michelson, A. M., & Yaniv, M. (1971) *J. Mol. Biol. 58*, 367–379.
Goddard, J. P., & Lowdon, M. (1978) *Eur. J. Biochem. 89*, 531–541.
Gupta, R. C., & Randerath, K. (1979) *Nucleic Acids Res. 6*, 3443–3458.
Isaacs, S. T., Chen, C.-K. J., Hearst, J. E., & Rapoport, H. (1977) *Biochemistry 16*, 1058–1064.
Isaacs, S. T., Hearst, J. E., & Rapoport, H. (1982) *J. Labelled Compd. Radiopharm.* (in press).
Jack, A., Ladner, J. E., & Klug, A. (1976) *J. Mol. Biol. 108*, 619–649.
Johnston, B. H., & Hearst, J. E. (1981) *Biochemistry 20*, 739–743.
Johnston, B. H., Johnson, M. A., Moore, C. B., & Hearst, J. E. (1977) *Science (Washington, D.C.) 197*, 906–908.
Kearns, D. R., & Schulman, R. G. (1974) *Acc. Chem. Res. 7*, 33–39.
Kim, S.-H., Quigley, G. J., Suddath, F. L., McPherson, A., Sneden, D., Kim, J. J., Weinzierl, J., & Rich, A. (1973) *Science (Washington, D.C.) 179*, 285–288.
Litt, M. (1969) *Biochemistry 8*, 3249–3253.
Ohashi, Z., Maeda, M., McCloskey, J. A., & Nishimura, S. (1974) *Biochemistry 13*, 2620–2625.
Rhodes, D. (1977) *Eur. J. Biochem. 81*, 91–101.
Rich, A., & RajBhandary, J. L. (1976) *Annu. Rev. Biochem. 45*, 805–860.
Ross, A., & Brimacombe, R. (1979) *Nature (London) 281*, 271–276.
Sommer, S. S. (1979) *Anal. Biochem. 98*, 8–12.
Sprinzl, M., Greuter, F., Spelzhaus, A., & Gauss, D. H. (1980) *Nucleic Acids Res. 8*, r1–r22.
Thompson, J. F., Wegnez, M., & Hearst, J. E. (1981) *J. Mol. Biol. 147*, 417–436.
Thompson, J. F., Bachellerie, J. P., Hall, K., & Hearst, J. E. (1982) *Biochemistry* (following paper in this issue).
Uhlenbeck, O. C., Chirikjian, J. G., & Fresno, J. R. (1974) *J. Mol. Biol. 89*, 495–504.
Wagner, R., & Garrett, R. A. (1978) *Nucleic Acids Res. 5*, 4065–4075.
Wintermeyer, W., & Zachau, H. G. (1975) *FEBS Lett. 58*, 306–309.
Wintermeyer, W., Thiebe, R., & Zachau, H. G. (1972) *Hoppe-Seyler's Z. Physiol. Chem. 353*, 1625–1632.
Wurst, R. M., Vournakis, J. N., & Maxam, A. M. (1978) *Biochemistry 17*, 4493–4499.
Yaniv, M., Favre, A., & Barrell, B. G. (1969) *Nature (London) 223*, 1331–1332.

Dependence of 4′-(Hydroxymethyl)-4,5′,8-trimethylpsoralen Photoaddition on the Conformation of Ribonucleic Acid†

John F. Thompson, Jean-Pierre Bachellerie,‡ Kathi Hall, and John E. Hearst*

ABSTRACT: The photoaddition of 4′-(hydroxymethyl)-4,5′,8-trimethylpsoralen (HMT) to different conformational states of RNA was studied. Poly(U), poly(A,U) (random copolymer), poly(A-U) (alternating copolymer), poly(A)·poly(U) (double stranded), and poly(U)·poly(A)·poly(U) (triple stranded) were reacted with HMT at different temperatures and salt concentrations. The conformation of the polymers was monitored by UV absorption and circular dichroism. It was found that the rate of HMT photoaddition changed dramatically at structural transitions in the RNA. The alternating copolymer poly(A-U) was found to have the highest rate of addition. Low salt and temperature produced maximal incorporation.

Psoralen and its derivatives have been used increasingly to study the structure of nucleic acids. Psoralen is a planar, aromatic molecule that can intercalate into the double helix and then photoreact with the 5,6 double bond of a pyrimidine. We have used a derivative of psoralen, 4′-(hydroxymethyl)-4,5′,8-trimethylpsoralen (HMT), which is both more reactive and more water soluble than the parent compound (Isaacs et al., 1977). HMT has two reactive sites that, with two photons, can cross-link opposite and adjacent bases to covalently link two strands. These cross-links can then be localized to provide information about the secondary and tertiary structure of a molecule. Electron microscopy has been used to map cross-links in 16S ribosomal RNA (Wollenzien et al., 1979) and fd virus (Shen et al., 1979), while more recently, monoadducts (Bachellerie & Hearst, 1982) and cross-links (Thompson et al., 1981; Rabin & Crothers, 1979) have been mapped to sequence resolution in smaller RNAs.

In order to take full advantage of this structural probe, it is necessary to find both the specificity and the optimal conditions for the reaction. It has been apparent for some time

† From the Department of Chemistry (J.F.T., J.-P.B., and J.E.H.), University of California, Berkeley, California 94720, and the Divisions of Chemical Biodynamics (J.F.T. and J.E.H.) and Biology and Medicine (K.H.), Lawrence Berkeley Laboratory, Berkeley, California 94720. *Received May 18, 1981.* This work was supported in part by National Institutes of Health Grant GM 11180, by an NIH Fogarty Fellowship to J.-P.B., by National Institutes of Health Grant GM 25936-01 to K.H., and by the Assistant Secretary for Environment, Office of Environmental Research and Development, Biomedical and Environmental Research Division of the U.S. Department of Energy under Contract No. W-7405-ENG-48.

‡ Present address: Centre de Recherche de Biochimie et Génétique Cellulaires du CNRS, 31062 Toulouse Cedex, France.

0006-2960/82/0421-1363$01.25/0